Optical Engineering

OpticalEngineering.SPIEDigitalLibrary.org

Feedback method and structure to improve the stability of the OFC-generated system based on electro-optic modulation

Xiangchuan Wang
Wei Wang
Dan Zhu
Angran Zhao
Weijia Ma
Simin Li
Shilong Pan

SPIE.

Xiangchuan Wang, Wei Wang, Dan Zhu, Angran Zhao, Weijia Ma, Simin Li, Shilong Pan, "Feedback method and structure to improve the stability of the OFC-generated system based on electro-optic modulation," *Opt. Eng.* **58**(8), 086102 (2019), doi: 10.1117/1.OE.58.8.086102.

Downloaded From: https://www.spiedigitallibrary.org/journals/Optical-Engineering on 07 Mar 2022
Terms of Use: https://www.spiedigitallibrary.org/terms-of-use

Feedback method and structure to improve the stability of the OFC-generated system based on electro-optic modulation

Xiangchuan Wang,[a] Wei Wang,[a] Dan Zhu,[a] Angran Zhao,[a] Weijia Ma,[b,*] Simin Li,[a] and Shilong Pan[a,*]
[a]Nanjing University of Aeronautics and Astronautics, Ministry of Education, Key Laboratory of Radar Imaging and Microwave Photonics, Nanjing, China
[b]Industry Development Promotion Center of Ministry of Industry and Information Technology of the People's Republic of China, Beijing, China

Abstract. A stability improved optical frequency comb (OFC) generation system based on a single integrated polarization multiplexing dual-drive Mach–Zehnder modulator is proposed. Due to the influence of the modulator bias drift on the spectra of the OFC, the amplitude of the OFC spectra would fluctuate with time, which seriously deteriorates the stability of the OFC. The effect of the modulator bias drift on the stability of the OFC is analyzed by theoretical analyses and numerical simulations. A feedback system is proposed to improve the OFC stability. The ratio between the total power of the OFC and the optical carrier power is used as the feedback parameter. In the proof-of-concept experiment, by using the feedback structure, the seven-line OFC stability is experimentally improved from being large than 3 dB within 1.5 h to being below 2 dB more than 4 h. © *2019 Society of Photo-Optical Instrumentation Engineers (SPIE)* [DOI: 10.1117/1.OE.58.8.086102]

Keywords: optical frequency comb; electro-optic modulation; stability; feedback.

Paper 190713 received May 23, 2019; accepted for publication Jul. 19, 2019; published online Aug. 6, 2019.

1 Introduction

Optical frequency combs (OFCs) are critically important for applications such as precision measurement,[1,2] optical sensing,[3] optical arbitrary waveform generation,[4] and microwave photonics signal processing,[5,6] etc. A large number of approaches have been proposed to generate OFCs, which can be generally divided into three categories: OFC generation based on nonlinearity effect,[7] mode-locked laser,[8] and external electro-optic modulation.[9] For the first one, broadband OFC generation can be achieved based on the optical nonlinearity effect. A 10-GHz OFC of 143 lines is generated with nonlinear effects in highly nonlinear fibers,[10] while a comb consists of about 70 lines at 1450 to 1650 nm is achieved based on the four-wave mixing effect in the aluminum nitride microring resonator.[11] However, OFC generation based on the nonlinearity effect suffers from frequency and amplitude noise, which degrades OFC stability. For approaches based on the mode-locked laser, by measuring and controlling parameters such as repetition rate, integral mode index, and carrier-envelope offset frequency, OFC can be obtained.[12] However, the line spacing of the OFCs generated based on the nonlinearity effect and the mode-locked laser is difficult to adjust online. To solve these problems, the OFC generation approaches based on electro-optic modulation have been proposed due to the high flexibility, low complexity, and coherent phase relations.[13–15] A seven-line OFC is obtained using only one RF source based on a single polarization modulator (PolM).[16] However, the optical signal needs to be divided into two independent paths and an erbium-doped fiber amplifier is used, which would increase the amplitude noise. An 11-line OFC is generated with a deviation of less than 1 dB by using a dual-drive Mach–Zehnder odulator (DMZM)[17] while cascaded PolMs-based structures have been proposed to generate OFC with 25 lines.[13] Recently, a flexible flat OFC generator based on a single integrated polarization multiplexing dual-drive Mach–Zehnder modulator (PM-DMZM)[18] is proposed where only one PM-DMZM is required, guaranteeing the simplicity. However, the stability of modulator-based OFC generation systems are widely affected by the bias drifting problem, which would greatly limit the OFC applications. Recently, we proposed a feedback structure to improve the stability of modulator-based OFCs.[19] However, only some preliminary simulation results were reported, which was insufficient to understand the approach in-depth.

In this work, comprehensive theoretical and experimental investigations are taken. The principle of the proposed system is given in Sec. 2, where the numerical simulation model is also established. A proof-of-concept experiment and discussion are carried out accordingly in Sec. 3 and is followed by the conclusion in Sec. 4. Based on the proposed feedback structure, the stability of the OFC generation system is greatly improved. The key significance of the technique is that a stability-enhanced OFC is obtained to promote the engineering process of the modulator-based OFC generating system. In addition, a flexible OFC can also be achieved because the proposed feedback method can be applied to the PM-DMZM or other type of modulators operating at any bias point.

2 Principle

The schematic diagram of the proposed system is shown in Fig. 1. An optical carrier with an angular frequency of ω_0 is sent into the PM-DMZM, where the optical signal is split

*Address all correspondence to Weijia Ma, E-mail: maweijia@idpc.org.cn; Shilong Pan, E-mail: pans@nuaa.edu.cn.

0091-3286/2019/$28.00 © 2019 SPIE

Downloaded From: https://www.spiedigitallibrary.org/journals/Optical-Engineering on 07 Mar 2022
Terms of Use: https://www.spiedigitallibrary.org/terms-of-use

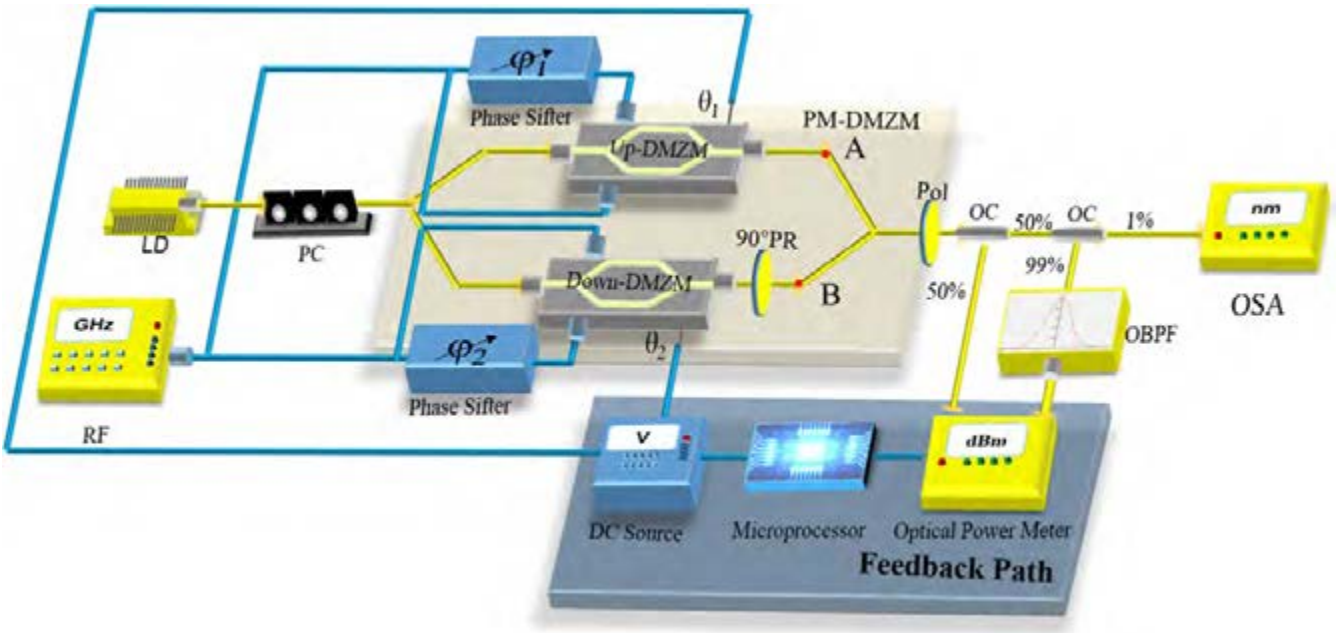

Fig. 1 Schematic diagram of the stability improved OFC generating system based on a PM-DMZM. LD, laser diode; PM-DMZM, polarization-multiplexing dual-drive Mach–Zehnder modulator; PR, polarization rotator; Pol, polarizer; PC, polarization controller; OC, optical coupler; OSA, optical spectrum analyzer; OBPF, optical bandpass filter.

into two parts with equal power. The light is modulated by an RF signal with a frequency of ω_m. The output of PM-DMZM can be theoretically described as follows:[18]

$$p_n(V_\pi) \propto 4E_0^2\Big\{J_n^2(\beta_1)\cos^2\alpha + J_n^2(\beta_2)\sin^2\alpha + J_n^2(\beta_1)\cos^2\left(\frac{\theta_2+n\varphi_2}{2}\right) + J_n(\beta_1)J_n(\beta_2)\sin 2\alpha \cdot \cos\left(\frac{n\varphi_1+\theta_1}{2}\right)\cos\left(\frac{n\varphi_2+\theta_2}{2}\right) \times \cos\left[\frac{n(\varphi_1-\varphi_2)+\theta_1-\theta_2}{2}\right]\Big\}, \quad (1)$$

where β_1 and β_2 are the modulation index at the up-DMZM and the down-DMZM, respectively, φ_1 and φ_2 are the phase difference between the two parts of the split RF signal in the upper and lower branches, θ_1 and θ_2 are the bias point at up-DMZM and down-DMZM, J_n is the n-th-order Bessel function of the first kind, α is the angle between the tunable polarizer's principal axis and the principal axis of the PM-DMZM. In the upper branch, the RF signal amplitude is V_{1m}, and up-DMZM biased at V_{bias1} has a half-wave voltage of $V_{\pi 1}$. Meanwhile, the RF signal applied at the down-DMZM with a half-wave voltage of $V_{\pi 2}$ has an amplitude of V_{2m}, and the bias voltage is set to be V_{bias2}. In addition, θ and β are given as

$$\beta = \pi V_m/V_\pi \quad \theta = \pi V_{bias}/V_\pi. \quad (2)$$

From Eqs. (1) and (2), it can be seen that the relative amplitude of the sidebands is decided by the values α, microwave amplitude V_m, and bias voltage V_{bias}. When the parameters are chosen to be as $V_{bias1} = 4.3$ V, $V_{bias2} = 4.7$ V, $\beta_1 = 2.4$, $\beta_2 = 3$, $\alpha = 2.25$, $\varphi_1 = 3.13$, $\varphi_2 = 3.13$, $V_{\pi 1} = V_{\pi 2} = 3.5$ V, a seven-line OFC can be generated as shown in Fig. 2(a). The flatness is about 1.067 dB. However, as the modulation indexes (β_1, β_2) and the bias points (θ_1, θ_2) will change gradually due to the RF power fluctuation and bias drift of the modulator, the OFC flatness will be deteriorated. As can be seen from Fig. 2(b), the flatness of the seven-line OFC will degrade to 7.32 dB when $\beta_1 = 2.8$, $\beta_2 = 3.4$, $\theta_1 = 4.5$, and $\theta_2 = 4.9$. Thus, a

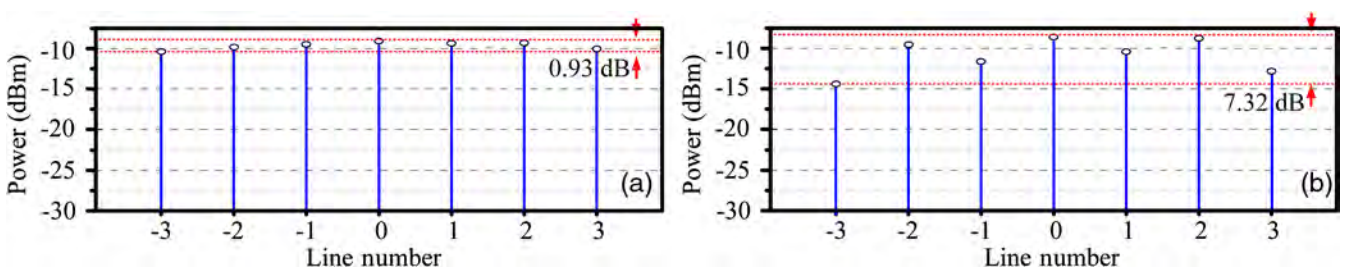

Fig. 2 Simulated results of the seven-line OFC: (a) when $\beta_1 = 2.4$, $\beta_2 = 3$, $\theta_1 = 3.8$, and $\theta_2 = 4.2$ and (b) when $\beta_1 = 2.8$, $\beta_2 = 3.4$, $\theta_1 = 4.5$, and $\theta_2 = 4.9$.

Downloaded From: https://www.spiedigitallibrary.org/journals/Optical-Engineering on 07 Mar 2022
Terms of Use: https://www.spiedigitallibrary.org/terms-of-use

feedback system to compensate for the variation of bias drift and RF power fluctuation is proposed to improve the stability of the OFC.

The proportion between the total optical power of the OFC and the optical carrier power is served as the feedback parameter, with the expression as follows:

$$F = \frac{\sum_{n=-\infty}^{n=\infty} p_n(\beta_u, \beta_d, \theta_u, \theta_d)}{p_0(\beta_u, \beta_d, \theta_u, \theta_d)}, \tag{3}$$

where $\beta_u = \beta_1 + \Delta\beta_1$, $\beta_d = \beta_2 + \Delta\beta_2$, $\theta_u = \theta_1 + \Delta\theta_1$, $\theta_d = \theta_2 + \Delta\theta_2$, $\Delta\beta_1$, and $\Delta\beta_2$ are the variation of β in the upper and lower branches and $\Delta\theta_1$ and $\Delta\theta_2$ are the variation of θ in the upper and lower branches, respectively. Since the two branches are in the same environment, the variation of modulation indexes and bias points can be approximated as the same value, i.e., $\Delta\beta_1 = \Delta\beta_2 = \Delta\beta$, $\Delta\theta_1 = \Delta\theta_2 = \Delta\theta$. Then, Eq. (3) can be rewritten as

$$F = \frac{\sum_{n=-\infty}^{n=\infty} p_n(\Delta\beta, \Delta\theta)}{p_0(\Delta\beta, \Delta\theta)}. \tag{4}$$

Figure 3(a) shows the relationship between the proportion F and the half-wave voltage of the PM-DMZM. The flatness of the OFC is 1.067 dB at the optimal operating point "Q" when both $\Delta\beta$ and $\Delta\theta$ are 0. In order to compensate for the change of $\Delta\beta$ and $\Delta\theta$, the bias voltage and microwave amplitude are controlled according to the value of F to make that the system work at point "Q." The brief program chart of the feedback method is shown in Fig. 3(b). At the first step, the value of F at "Q" point is measured and recorded when the OFC is generated. Then, the value of F is monitored in real

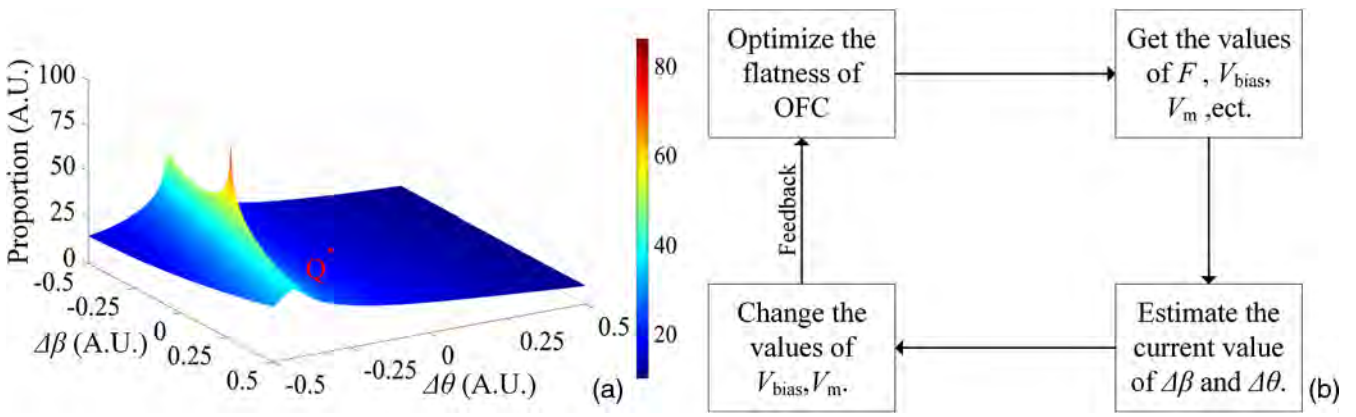

Fig. 3 (a) The relationship of the proportion F with $\Delta\beta$ and $\Delta\theta$ and (b) the brief program chart of the feedback method.

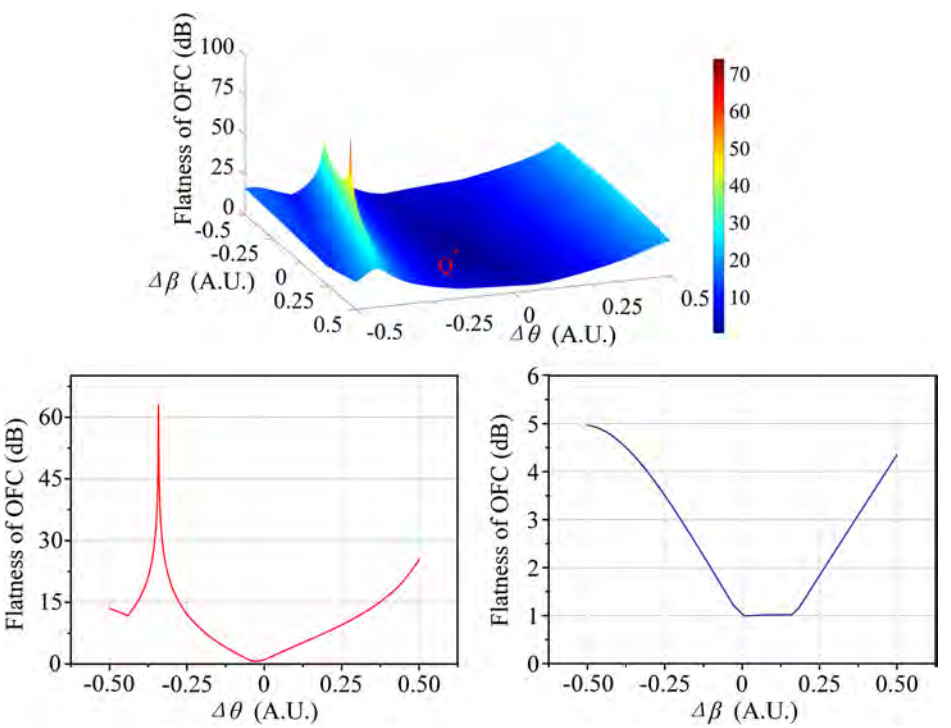

Fig. 4 The relationship of (a) the flatness of the seven-line OFC versus $\Delta\beta$ and $\Delta\theta$, (b) versus $\Delta\theta$ ($\Delta\beta = 0$), and (c) versus $\Delta\beta$ ($\Delta\theta = 0$).

Downloaded From: https://www.spiedigitallibrary.org/journals/Optical-Engineering on 07 Mar 2022
Terms of Use: https://www.spiedigitallibrary.org/terms-of-use

time. According to the relationship shown in Fig. 3(a), the changing trend of $\Delta\beta$ and $\Delta\theta$ can be obtained. To achieve system stability, the parameter F should be always close to "Q." Thus, θ and β should be unchanged. Then, the values of V_m and V_{bias} are adjusted to compensate for the change of $\Delta\beta$ and $\Delta\theta$ accordingly. Accordingly, the feedback loop is formed while the flatness of OFC is optimized.

In the simulation, the three-dimensional image of the relationship of flatness of OFC with $\Delta\beta$ and $\Delta\theta$ is shown in Fig. 4(a). If only the power of the RF signal is regarded as the control parameter ($\Delta\beta = 0$), the worst flatness of the seven-line OFC versus $\Delta\theta$ would exceed 60 dB as shown in Fig. 4(b). If only the bias voltage V_{bias} is regarded as the control parameter ($\Delta\theta = 0$), the worst flatness of the seven-line OFC versus $\Delta\beta$ is below 5 dB as shown in Fig. 4(c). As shown in Figs. 4(b) and 4(c), the effect of the parameter $\Delta\beta$ on the flatness is much less than the effect of the parameter $\Delta\theta$ on the flatness. Therefore, the effect of the parameter $\Delta\beta$ on the flatness can be ignored when the RF power fluctuation is also much smaller than the bias drift, which is common in practice.

3 Experimental Results and Discussion

A proof-of-concept experiment based on the scheme shown in Fig. 1 is carried out. The CW light from the LD (TeraXion NLL04) has a wavelength of 1550.548 nm. The PM-DMZM (Fujitsu FTM7980EDA) has a bandwidth of 20 GHz and a half-wave voltage of 3.5 V. A microwave signal generator (Keysight N5183B) generates the modulated RF signal.

By setting the powers of the modulated 10-GHz RF signal in the upper and lower branches to be 22.8 and 24.1 dBm, respectively, $V_{\text{bias1}} = 4.07$ V, $V_{\text{bias2}} = 4.22$ V, a seven-line OFC with the flatness of 0.985 dB is successfully generated as shown in Fig. 5.

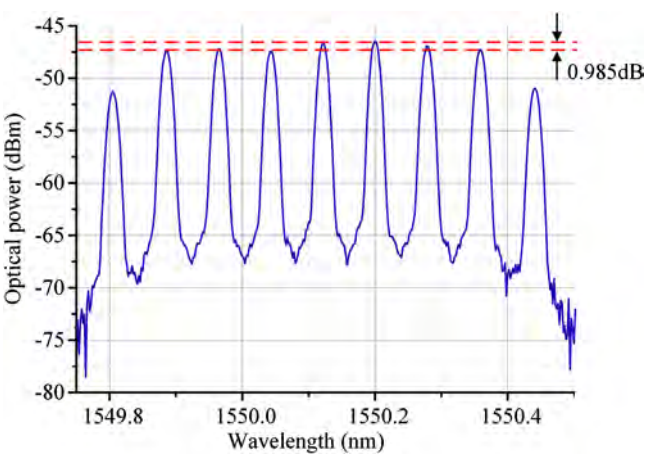

Fig. 5 The experimentally measured optical spectra of the generated seven-line OFC.

As the effect of RF power fluctuation on the amplitude stability is very small, only the effect of bias drift is considered. Figure 6 shows the relationship of the flatness of seven-line OFC versus $\Delta\theta$ and the relationship of $\Delta\theta$ and the proportion between the optical power of OFC and the optical carrier power. It can be seen that the flatness of generated seven-line OFC is 0.985 dB when $\Delta\theta$ is 0 while the proportion F is 23.78 dB. The flatness would be deteriorated from 0.985 to 3.446 dB when $\Delta\theta$ changes from 0 to 0.5. Based on the brief program chart in Fig. 3, the feedback system is experimentally established. We measure the value of F regularly and compare it with the proportion at point "Q" after each measurement. If the value of F is greater than the proportion at point "Q," V_{bias} is increased to compensate for the variation of $\Delta\theta$. In the same way, if the measured F value is less than the proportion at "Q" point, the V_{bias} would be decreased. The adjusting speed and step of the feedback structure are 15 Sa/min and 0.05 V, respectively, in the experiment.

Figure 7 shows the changing process of the bias voltages and the proportion value within 4 h with the feedback structure. Among the range of 0 to 70 min as shown in Fig. 7(a), the slope of the bias voltage is greater than zero, while for the time beyond 70 min, it is monotonically decreasing. It means that $\Delta\theta$ decreases gradually from 0 to 70 min and increases during 70 to 240 min according to Eq. (2). In addition, the change of the proportion F is also measured. In Fig. 7(b), the values of the proportion curve are around 23.87 dB with fluctuation of about 0.1 dB. It means that the proportion can be adjusted around the optimal operating point, showing good performance of the OFC stability by introducing the feedback structure.

In order to further test the effectiveness of the feedback system, the flatness of the OFCs is captured within 4 h. The powers of the modulated 10-GHz RF signal in the upper and lower branches are initially set to be 20.9 and 23.3 dBm

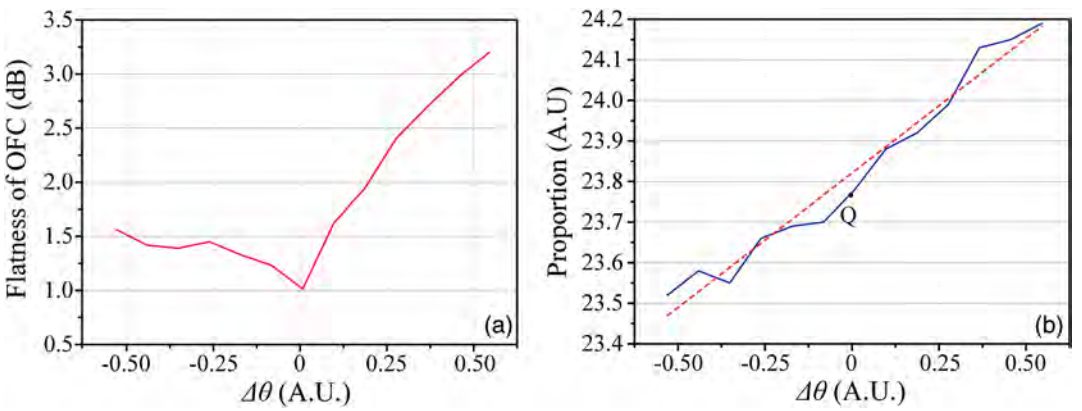

Fig. 6 The relationship of (a) the flatness of the seven-line OFC versus $\Delta\theta$ and (b) the relationship of the proportion F versus the $\Delta\theta$ value.

Downloaded From: https://www.spiedigitallibrary.org/journals/Optical-Engineering on 07 Mar 2022
Terms of Use: https://www.spiedigitallibrary.org/terms-of-use

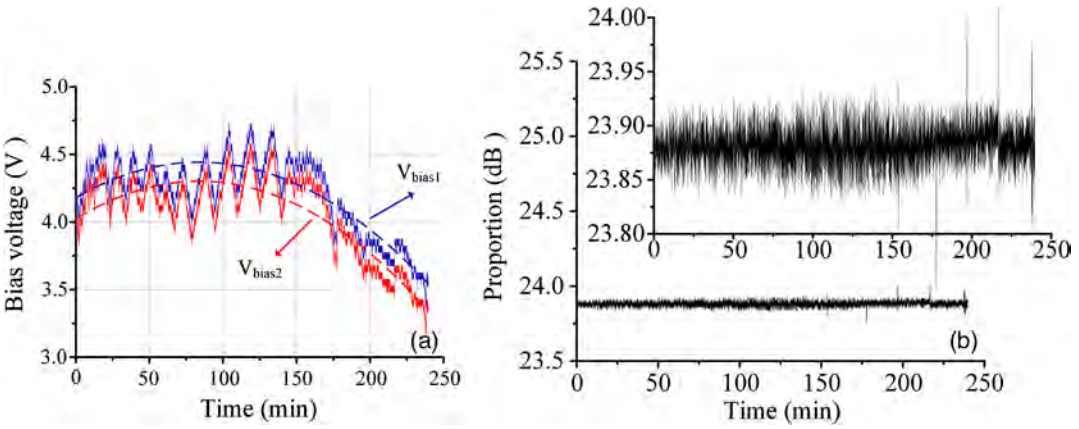

Fig. 7 Slopes of (a) the bias voltages versus the time and (b) the proportion versus time (The inset is the magnified graph zoomed in between 23.8 and 24 dB).

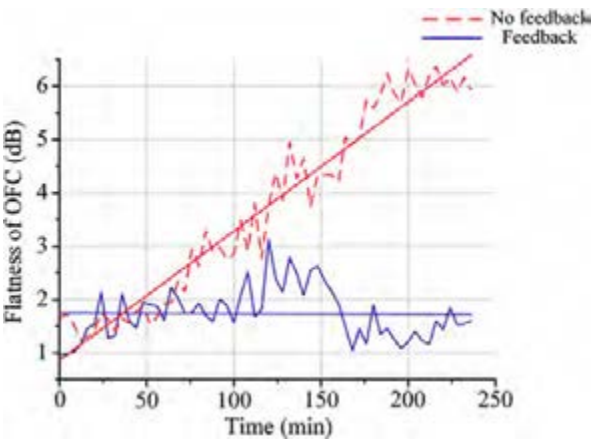

Fig. 8 The experimentally measured OFC flatness versus time with/without using the feedback control.

while the bias voltages are set as $V_{\text{bias1}} = 3.99$ V, $V_{\text{bias2}} = 3.89$ V. Another seven-line OFC is successfully generated with the flatness of 1.641 dB. Sixty flatness samples are captured within 4 h with/without the feedback system as shown in Fig. 8. The flatness of OFC can be controlled below 2 dB when the feedback system works. On the contrary, the flatness of OFC is deteriorated to be large than 3 dB after 90 min without the feedback system. Thus, it can be seen that by introducing the proposed feedback control system, the stability of the OFC generated based on electro-optical modulators can be greatly improved. It should be noted here, although experimental results were only captured in 4 h, the proposed system can maintain the stability a longer time as the trend of the flatness curve with feedback structure is still gentle after 4 h.

4 Conclusion

In conclusion, a feedback structure was proposed and demonstrated to improve the stability of OFC generated based on electro-optical modulators. The proportion between the total optical power and the optical carrier power of OFC is used as the feedback parameter. A proof-of-concept experiment is taken. Using the feedback structure, the seven-line OFC stability is improved from being large than 3 dB within 1.5 h to being below 2 dB more than 4 h. The scheme can find applications in microwave photonic systems where the OFCs with good stability are highly required, such as the radar, electronic warfare systems, and so on.

Acknowledgments

This work was supported in part by the National Natural Science Foundation of China (Nos. 61605077 and 61527820), Jiangsu Provincial "333" Project (BRA2018042), the Fundamental Research Funds for the Central Universities (NT201911), and Young Elite Scientists Sponsorship Program by CAST (2018QNRC001).

References

1. J. Lee et al., "Time-of-flight measurement with femtosecond light pulses," *Nat. Photonics* **4**(10), 716–720 (2010).
2. M. Xue et al., "Wideband optical vector network analyzer based on optical single-sideband modulation and optical frequency comb," *Opt. Lett.* **38**(22), 4900–4902 (2013).
3. T. Minamikawa et al., "Strain sensing based on strain to radio-frequency conversion of optical frequency comb," *Opt. Express* **26**(8), 9484–9491 (2018).
4. Z. Jiang et al., "Optical arbitrary waveform processing of more than 100 spectral comb lines," *Nat. Photonics* **1**(8), 463–467 (2007).
5. P. J. Delfyett et al., "Optical frequency combs from semiconductor lasers and applications in ultrawideband signal processing and communications," *J. Lightwave Technol.* **24**(7), 2701–2719 (2006).
6. S. Pan et al., "Satellite payloads pay off," *IEEE Microwave Mag.* **16**(8), 61–73 (2015).
7. P. Del'Haye et al., "Optical frequency comb generation from a monolithic microresonator," *Nature* **450**(7173), 1214–1217 (2007).
8. R. Holzwarth et al., "Optical clockworks and the measurement of laser frequencies with a mode-locked frequency comb," *IEEE J. Quantum Electron.* **37**(12), 1493–1501 (2001).
9. R. Wu et al., "Generation of very flat optical frequency combs from continuous-wave lasers using cascaded intensity and phase modulators driven by tailored radio frequency waveforms," *Opt. Lett.* **35**(19), 3234–3236 (2010).
10. T. Yang et al., "Comparison analysis of optical frequency comb generation with nonlinear effects in highly nonlinear fibers," *Opt. Express* **21**(7), 8508–8520 (2013).
11. H. Jung et al., "Optical frequency comb generation from aluminum nitride microring resonator," *Opt. Lett.* **38**(15), 2810–2813 (2013).
12. S. A. Diddams, "The evolving optical frequency comb," *J. Opt. Soc. Am. B* **27**(11), B51–B62 (2010).
13. C. He et al., "Ultraflat optical frequency comb generated based on cascaded polarization modulators," *Opt. Lett.* **37**(18), 3834–3836 (2012).
14. X. Yan et al., "Fully digital programmable optical frequency comb generation and application," *Opt. Lett.* **43**(2), 283–286 (2018).
15. I. Demirtzioglou et al., "Frequency comb generation in a silicon ring resonator modulator," *Opt. Express* **26**(2), 790–796 (2018).
16. S. Ozharar et al., "Ultraflat optical comb generation by phase-only modulation of continuous-wave light," *IEEE Photonics Technol. Lett.* **20**(1), 36–38 (2007).
17. N. Yokota et al., "Harmonic superposition for tailored optical frequency comb generation by a Mach-Zehnder modulator," *Opt. Lett.* **41**(5), 1026–1029 (2016).

Downloaded From: https://www.spiedigitallibrary.org/journals/Optical-Engineering on 07 Mar 2022
Terms of Use: https://www.spiedigitallibrary.org/terms-of-use

18. D. Zhu et al., "Thirteen coherent comb lines generated by a single integrated modulator," *Opt. Eng.* **57**(2), 026116 (2018).
19. W. Wang et al., "A feedback system for the stability improvement of optical frequency comb generating system based on a single integrated PM-DMZM," in *17th Int. Conf. Opt. Commun. and Networks (ICOCN2018)* (2019).

Xiangchuan Wang received his BEng degree in automation and his PhD in microelectronics and solid-state electronics from Nanjing University, China, in 2009 and 2015, respectively. Currently, he is with the Key Laboratory of Radar Imaging and Microwave Photonics (Nanjing University of Aeronautics and Astronautics), Ministry of Education, China, as a lecturer. His current research interests are in microwave photonic measurement and optical fiber sensing technologies.

Wei Wang is a postgraduate of Key Laboratory of Radar Imaging and Microwave Photonics (Nanjing University of Aeronautics and Astronautics), Ministry of Education, China. His research has focused on microwave photonics.

Dan Zhu received her BS and PhD degrees in electronics engineering from Tsinghua University, Beijing, China, in 2004 and 2009, respectively. In May 2011, she joined the Key Laboratory of Radar Imaging and Microwave Photonics (Nanjing University of Aeronautics and Astronautics), Ministry of Education, China, where she is now an associate professor. Her current research interests include microwave photonic signal generation and processing.

Angran Zhao is a postgraduate of Key Laboratory of Radar Imaging and Microwave Photonics (Nanjing University of Aeronautics and Astronautics), Ministry of Education, China. His research has focused on high dynamic range analog photonic links and photonics-based imaging radar.

Weijia Ma received his PhD from Harbin Engineering University, China, in 2012. Currently, he is with the Industry Development Promotion Center of Ministry of Industry and Information Technology of the People's Republic of China.

Simin Li received her bachelor's and a PhD from Nanjing University, China, in 2009 and 2014, respectively. Currently, she is working in the Key Laboratory of Radar Imaging and Microwave Photonics (Nanjing University of Aeronautics and Astronautics), Ministry of Education, China. Her current research interest is in integrated microwave photonics.

Shilong Pan received his BS and PhD degrees in electronics engineering from Tsinghua University, Beijing, China, in 2004 and 2008, respectively. From 2008 to 2010, he was a "Vision 2010" postdoctoral research fellow in the Microwave Photonics Research Laboratory, University of Ottawa, Canada. Currently, he is a full professor and executive director at the Key Laboratory of Radar Imaging and Microwave Photonics (Nanjing University of Aeronautics and Astronautics), Ministry of Education, China.

Downloaded From: https://www.spiedigitallibrary.org/journals/Optical-Engineering on 07 Mar 2022
Terms of Use: https://www.spiedigitallibrary.org/terms-of-use